

# The simulation of TanSat measurements in terrestrial CO<sub>2</sub> flux estimation



J.Wang<sup>1</sup>, Y.Liu<sup>1</sup>, L.Feng<sup>2</sup>, D.Yang<sup>1</sup>

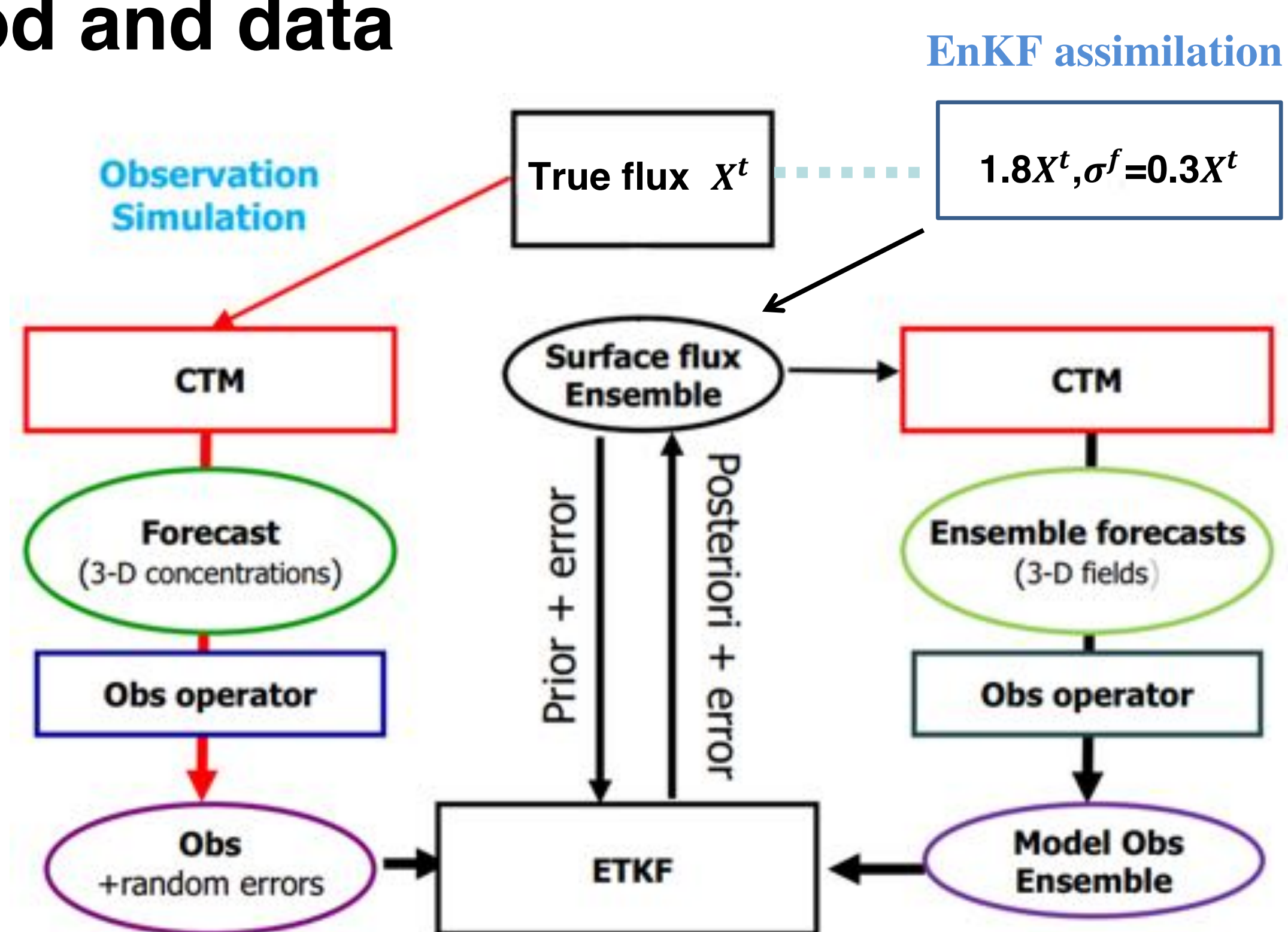
<sup>1</sup> LAGEO, Institute of Atmospheric Physics, Chinese Academy of Sciences, Beijing 100029, China

<sup>2</sup> School of GeoSciences, University of Edinburgh, King's Buildings, Edinburgh, EH9 3JN, UK

## 1 Introduction

It's essential to know the precise sources and sinks of surface CO<sub>2</sub> flux generated by human and natural activities more accurately. The inverse approach models ("top-down") using atmospheric CO<sub>2</sub> observations and atmospheric transport model have been applied to infer the mean spatial distribution of CO<sub>2</sub> fluxes. With the satellite measurements, we can reduce many uncertainties in carbon flux estimation. China's carbon dioxide observation satellite (TanSat) will be launched in the end of 2016. We want to know the potential contribution of TanSat measurements on the terrestrial surface carbon flux estimation. In this study, we evaluate the potential effect of the forthcoming TanSat measurements for characterizing terrestrial CO<sub>2</sub> fluxes through the ensemble Kalman Filter (EnKF) developed by L.Feng. We show that TanSat measurements significantly improve the estimation of surface CO<sub>2</sub> fluxes. On the other hand, seasonally depended error reduction and seasonal cycles of CO<sub>2</sub> surface flux in different Transcom 3 regions are presented by the inversion model.

## 2 Method and data



### • Chemistry transport model : GEOS-Chem

horizontal resolution of 4°(latitude) 5°(longitude) with 47 vertical levels that span from the surface to the mesosphere with typically 35 levels in the troposphere.  
 meteorological analyses GEOS-5  
 boundary condition

- 1) 3-hourly fluxes for the terrestrial biosphere
- 2) monthly ocean fluxes
- 3) monthly biomass burning fluxes
- 4) monthly fossil fuel emissions

### • TanSat measurements

32 day cycle (16 nadir (only over land) + 16 glint)  
 instrument error  
 random error (Gaussian distribution, mean=0, Standard deviation = 1 ppm)  
 system error (use twice as the system error)

### • Screening cloud and aerosol (AOD > 0.3) contamination

3 hourly ECMWF probability density functions (PDFs)  
 aerosol optical depths (AODs), derived from the MODIS and MISR instruments

### • Simulation run

Prior flux: 1.8 \* true flux  
 Prior flux uncertainty: 0.3 \* true flux

## 3 Result

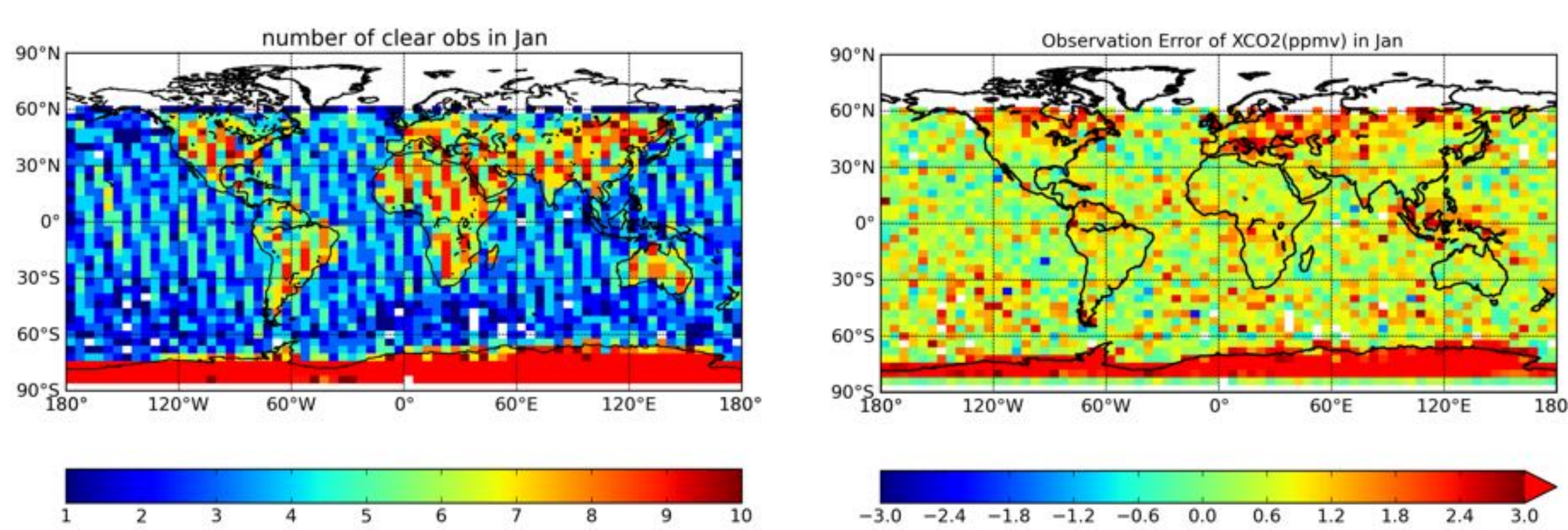


Fig 1 Observation numbers and errors in a 32-day cycle (16-day nadir + 16-day glint) in a 4° × 5° grid (from 2009.01.01-2009.02.01)

We get a posterior terrestrial flux of 7.79 ± 0.82 GtC, improved from a priori surface land flux of 11.89 ± 1.88 GtC, with a positive bias of 1.19 GtC to the true flux 6.60 GtC and the uncertainty reduction is about 56%. When we just consider the instrument error, the posterior flux only has a 0.09 GtC bias and the uncertainty reduction reach to 86%. For the posterior flux is sensitive to the satellite measurements, so we should have a strict control of retrieval data when we use the real satellite XCO<sub>2</sub>.

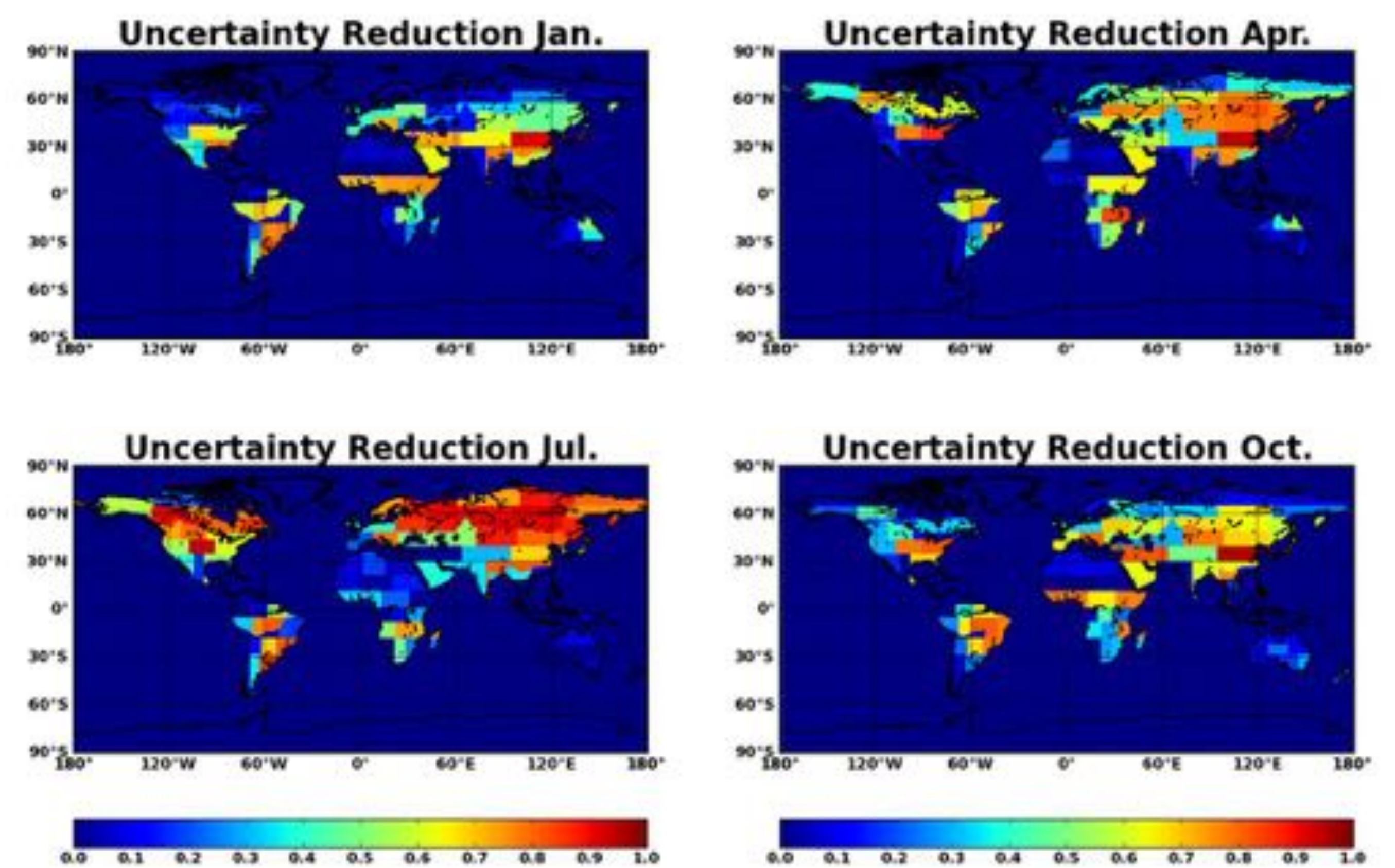


Fig2 Regional uncertainty error reduction for different seasons

The magnitude of uncertainty reduction is related to both the prior flux errors and the observations coverage. In winter of northern hemisphere especially latitude greater than 50°N, the uncertainty reduction is very small, but the error reduction can reach to more than 80% in summer. The measurements distribution plays an important role. For every month in the year for regions between 30°S and 30°N, the number of observations have little difference, the prior flux errors play an important role.

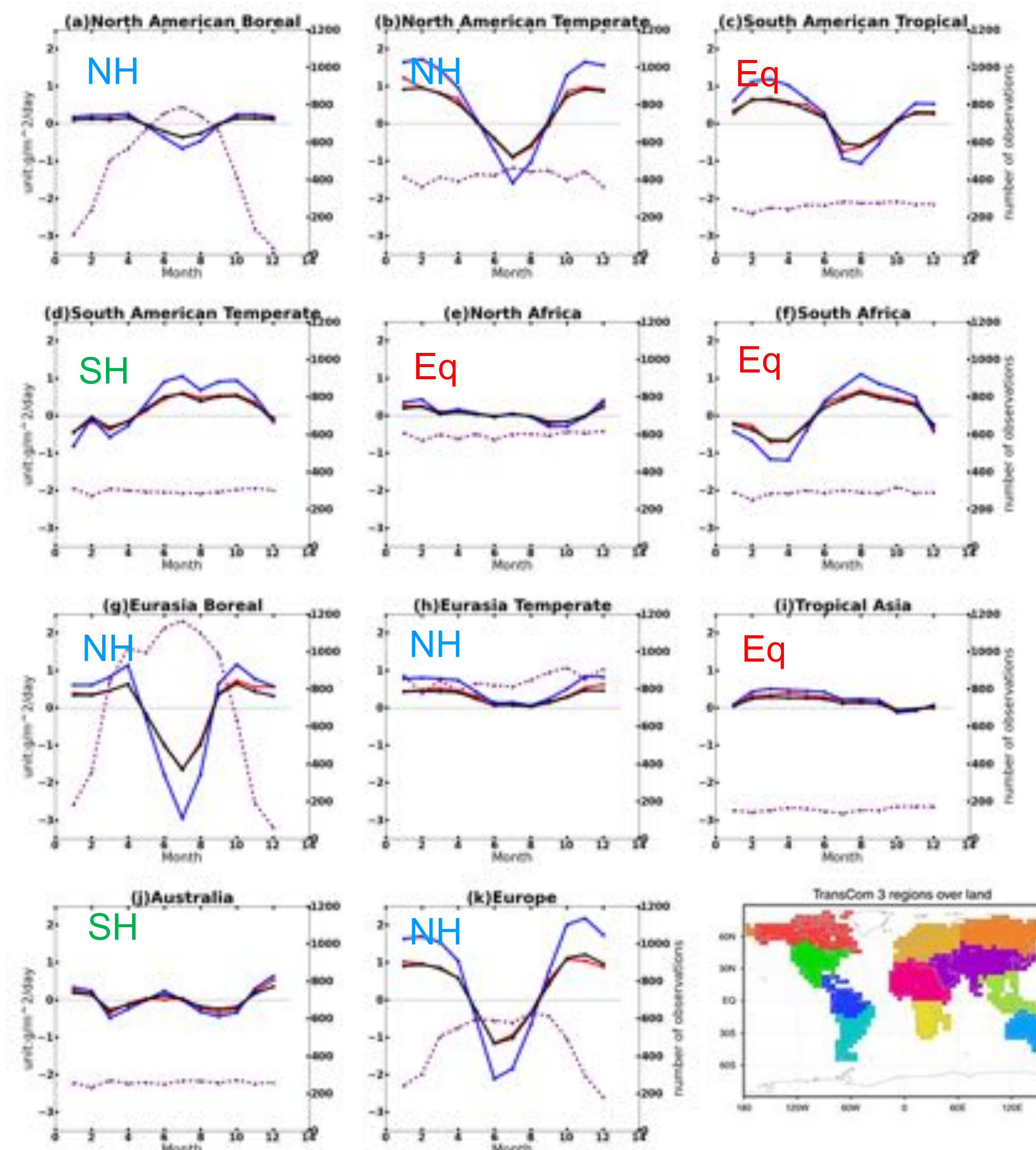


Fig 3 Seasonal cycle comparison among the true flux (black), the prior flux (blue) and the posterior flux (red) at 11 TransCom 3 land regions; purple line presents the total number of simulated TanSat observations at each region of a month (right y-axis)

The north hemisphere (a), (g), (k) have a large amount observation numbers in summer and relatively scarce numbers in winter. The observation numbers of regions in mid-low latitudes don't change with season variation, but for the region between 30°S and 30°N ((c), (e), (f), (i)), the satellite data are little than other regions due to the cloud contamination in rain season and aerosol contamination in dry season.

The true flux, prior flux and posterior flux have the same seasonal cycle phase, and the high latitude regions have larger amplitude. The northern hemisphere regions ((a), (b), (g), (k), (h)) have obvious seasonal cycle, from May to September are mainly sink of flux and from October to April are mainly source of flux. The flux of tropical region (i) don't change with season variation. The regions d, f, g in the south hemisphere almost have the opposite seasonal variation with north hemisphere.

## Reference

- Feng L, Palmer P I, H. Bösch, et al. Estimating surface CO<sub>2</sub> fluxes from space-borne CO<sub>2</sub> dry air mole fraction observations using an ensemble Kalman Filter[J]. Atmospheric Chemistry & Physics, 2009, 9(6):2619-2633.
- Chevallier F, Bréon F M, Rayner P J. Contribution of the Orbiting Carbon Observatory to the estimation of CO<sub>2</sub> sources and sinks: Theoretical study in a variational data assimilation framework[J]. Journal of Geophysical Research Atmospheres, 2007, 112(D9):139-155.
- Liu J. Carbon monitoring system flux estimation and attribution: impact of ACOS-GOSAT XCO<sub>2</sub> sampling on the inference of terrestrial biospheric sources and sinks[J]. Tellus Series B-chemical & Physical Meteorology, 2014, 66(3):78-82.